Spectral Analysis of DNA Superhelical Dynamics from Molecular Minicircle Simulations

Jeremy D. Curuksu[1,2]
[1)]*Amazon.com, Inc., New York, NY 10001, USA*
[2)]*Center for Data Science, New York University, New York, NY 10011, USA*

(*Electronic mail: curukj@amazon.com)

(Dated: 21 June 2023)

Torsional and bending deformations of DNA molecules often occur *in vivo* and are important for biological functions. DNA "under stress" is a conformational state which is by far the most frequent state during DNA-protein and gene regulation. In DNA minicircles of length < 100 base pairs the combined effect of torsional and bending stress can cause local unusual conformations, with certain base pair steps often absorbing most of the stress, leaving other steps close to their relaxed conformation. To better understand the superhelical dynamics of DNA under stress, molecular simulations of 94 bp minicircles with different torsional linking numbers were interpreted using Fourier analyses and principal component analyses. Sharp localized bends of nearly 90° in the helical axis were observed, which in turn decreased fluctuations of the rotational register and help redistribute the torsional stress into writhe i.e., superhelical turn up to 360°. In these kinked minicircles, only two-thirds of the DNA molecule bends and writhes, the remaining segment stays close-to-straight and preserves a conformational flexibility typical of canonical B-DNA (bending of $39° +/-17°$ distributed parsimoniously across 36 bp) which was confirmed and visualized by principal component analysis. These results confirm that stressed DNA molecules are highly heterogeneous along their sequence, with segments designed to locally store and release stress so that nearby segments can stay relaxed.

I. INTRODUCTION

The conformational flexibility for DNA fragments of length at or above 100 base pairs (bp) is often well described by a model accounting only for linearly elastic deformations, but the combined effect of torsional and bending stresses can cause local unusual conformations[1]. Cyclization assays and atomic force microscopy have both indicated that DNA bending energy alone is sufficient to induce local unusual conformations in minicircles of length up to 85 bp[2], and when combined with torsional stress in minicircles up to 339 bp[1,3].

Molecular dynamics (MD) simulations of DNA fragments under torsional stress[4] and bending stress (e.g., DNA minicircles as in[1,5,6]) have suggested the spontaneous occurrence of sharp localized twist and bent conformations. A 94 bp sequence is often chosen because it imposes the typical level of curvature observed in nucleosomal DNA *in vivo*, and it is also the length of the DNA fragments that had the highest cyclization probability in the experimental results that first indicated a unexpectedly high flexibility of DNA on length scales shorter than its persistence length[7,8]. The occurence of "kinked" conformations in DNA could explain these experiments, and even though such detailed conformations cannot directly be observed using existing experimental technologies, computer simulations give us an opportunity to describe in details the different kinds of local conformations that most likely occur in nature. DNA kinks have since been reported in many more molecular simulations of DNA[1,3,9–11].

In this paper, the results of all-atom MD simulations for 94 bp minicircles are interpreted using Fourier analyses and principal component analyses. These minicircles have three different linking numbers (underwound, relax, and overwound), different water models (TIP3P[12] and SPC/E[13]), and different physiological concentration of ions with respect to minimal salt. The results help understand the local confirmations and the more global, superhelical dynamics that characterize DNA under bending and torsional stress. Sharp localized bends of nearly 90° in the helical axis were observed in the torsionally stressed minicircles but not in the torsionally relaxed ones, in agreement with previous experimental and theoretical work[1,2]. The DNA kinks observed in overwound minicircles are not associated with unusual DNA backbone substates, but are strongly associated with the global minicircle structure and dynamics. These kinks decrease fluctuations of the rotational register and help redistribute the torsional stress into global superhelical turns (writhe). Most interestingly, only two-thirds of the minicircle structure bends and writhes, the remaining segment preserves a conformational flexibility typical of canonical B-DNA. This was measured and explicitly visualized by principal components analysis.

A. Material and Methods

A circularized DNA fragment of 94 base pairs with three different values of torsional load and an otherwise regular superhelical structure was built using JUMNA (JUnction Minimization of Nucleic Acids[14]) for the following sequence (as in[5]): GGCCGGGTCG TAGCAAGCTC TAGCACCGCT TAAACGCACG TACGCGCTGT CTACCGCGTT TTAACCGCCA ATAGGATTAC TTACTAGTCT CTAC.

This is a closed, planar minicircle with a standard helical rise of 3.38 Å and a helical twist that was set to three different values, 30.6°, 34.5°, and 38.3° respectively, corresponding to a linking number (Lk) of 8, 9, and 10. The linking number Lk is a mathematical invariant that describes the linking of closed curves in three-dimensional space and represents the number of times that two curves wind around each other, assuming no superhelical turn (writhe, see below). The two curves here are

the two strands of the DNA double helix, and as long as there is no writhe such as in the initial structure built by JUMNA, the linking number is directly proportional to the cumulative inter-base pair twist. The linking numbers of 8, 9 and 10 correspond to underwound, relaxed and overwound B-DNA conformations, respectively.

The superhelical dynamics can be measured by the time evolution of the writhe number $\mathrm{Wr}_{(t)}$, which amounts for the wrapping of the double helix on itself and was obtained from the White's formula[15]:

$$\mathrm{Wr}_{(t)} = \mathrm{Lk} - \theta_{(t)}$$

where Lk is the linking number, a fixed value for any given closed DNA molecule as long as no strand disruption accounts for their crossing, and $\theta_{(t)}$ is the twist number at time t obtained by computing the integral of the bp twist $\tau(s)$ along the minicircle contour line s:

$$\theta = \frac{1}{2\pi}\,\tau(s)\,ds$$

Note a writhe number Wr of exactly "1" is equivalent to an amount of superhelical wrapping equal to 360°.

Each starting structure was refined by minimizing the total potential energy of the molecular system in JUMNA. A first triplet of systems (Lk = 8, 9, and 10) was created by adding an octahedral periodic box of explicit TIP3P water molecules[12] and potassium (K+) ions in concentration sufficient to neutralize DNA phosphate negative charges (called "minimum salt" in the literature). Another triplet of systems (again Lk = 8, 9, and 10) was also created by replacing the TIP3P water model by SPC/E[13] and adding an extra 150 mM of potassium chloride (KCl) i.e., 140 K+ and 140 Cl- ("physiological conditions"). Other water and salt setup were explored too, such as minimal salt combined with the SPC/E water model. Molecular dynamics simulations were all performed with the AMBER 10 suite of programs (PMEMD module[16]) and the parmbsc0 force field[5]. Each system was equilibrated by a series of energy minimizations and short MD runs ($<$ 1ns). The production runs consisted of 100 ns unrestrained MD simulations in an NPT ensemble (see[1] for more context).

The analysis of the MD trajectories contains two parts, corresponding to an examination at the bp level and then a follow-up of the dynamics in term of global shape i.e., the superhelical dynamics. Conformational frames along the trajectories were saved every 1 ps and analyzed with CURVES+[17] both to obtain helical parameter and backbone torsion angle time series. CURVES+ was also used to compute the overall bend angle imposed by kinks that emerged in the simulations (sharp localized bend in the superhelix), by calculating two linear axes for the 10 bp segments preceding and following the observed kink, and computing the angle between these axes.

We further characterized the global shape of DNA minicircles using spectral analyses. First, the time evolution of the rotational register was obtained by a Fourier analysis of the helical roll angle distribution along the DNA sequence[18]. This is an harmonic decomposition in space, not in time: in each conformational frame, a Fourier analysis in polar coordinates can decompose the 94 bp signal into 48 scaled cosine functions (i.e., $94/2+1$), each with a specified magnitude and a phase shift. In a planar B-DNA minicircle the cosine function of highest magnitude always corresponds a sharp peak in the frequency domain (Fig. 5a) which is equal to the linking number (Fig. 5b). Its bandwidth corresponds to the number of cycles (where a *cycle* is a complete helical turn of 360°) over the length of the DNA sequence. This dominant cosine function corresponds to a function filtered from noise (local fluctuations at the bp level) that describes the periodic curvature along the double helix, assuming maxima and minima point toward the center of a planar minicircle. The phase parameter of this function amounts for rotation of the double helix around it own superhelical axis, called the *rotational register*. More details on the rotational register in the context of circularized DNA can be found in[5,19].

Finally, a Principal Component Analysis (PCA) of the conformational fluctuations in cartesian coordinates was carried out. Two separate PCAs were carried out, one on the phase of the trajectories prior to kink events occured, and one on the following phase where DNA molecules contain kinks (as mentioned above, kinks are sharp localized bends in the superhelix). For each phase, the corresponding trajectory was projected onto the first 50 eigenvectors within the PTRAJ module of AMBER 10[16]. By visually inspecting the eigenspectrum, the first few dominant modes were selected. The Interactive Essential Dynamics software[20] was used to visualize conformational frames along these modes and to characterize the global shape of minicircles when kinks occur.

B. Results

1. *Overwound DNA minicircles*

In this section we describe two MD trajectories of 94 bp minicircle with Lk = 10. At the equivalent torsional stress in[5], two types of kink occurred at two different positions in the minicircle. In type I kink a single bp step completely unstacks leading to a roll value of the order of 90°, with little disturbance of the neighborhood. In type II kink three successive bp are involved and the Watson-Crick hydrogen bonding of the central bp is broken such that each base stacks on its 5' neighbour.

The minicircle simulation called TK10 corresponds to minimal salt (K+ counterions) with the TIP3P water model, and the one called SKC10 is a simulation with 150 mM KCl and the SPC/E water model (Fig. 1). Both TK10 and SKC10 evolve toward a characteristic shape referred to as a swiss-roll in[5], where a close-to-straight segment of approximately 36 bp is capped at either end with kinks and joined to the remaining highly writhed S-shaped segment. A noticeable difference is that while two type II kinks are observed in TK10, a type I and type II kinks are observed in SKC10 (Fig. 2).

The type I kink in SKC10 appears at a CG bp step early in the simulation (10 ns, see table I) and closely resembles that originally described in 1975 by Francis Crick and Aaron Klug[21] with a roll angle close to 90° directed toward the local minor groove.

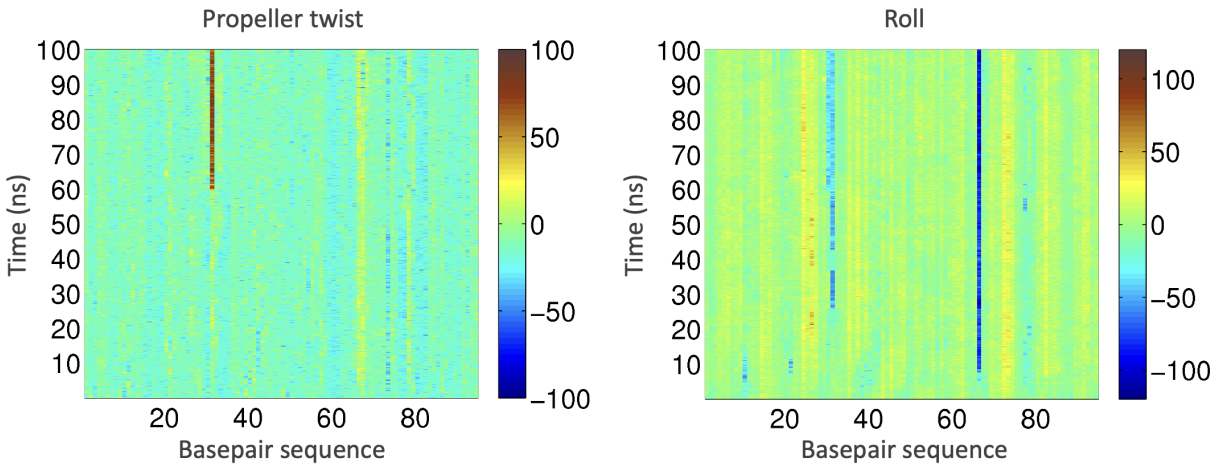

FIG. 1. Time evolution of bp propeller (left) and roll (right) in the overwound minicircle (Lk = 10) simulated with the SPC/E water model and 150 mM KCl. Base pairs (for propeller) and base pair steps (for roll) are numbered from left to right along the horizontal axis. Simulation time increases upward along the vertical axis. The color bar indicates the angular value in degrees.

TABLE I. Conformational deformations observed in each simulation.

Simulate [a]	Base pair step index	Base pair step	Start-end (ns)	Type of deformation	Bend angle [b] (degrees)
SKC10	66	CG	10-100	Type I kink	108 (9)
	30/31	TTA	60-100		109 (15)
TK10	47/48	CTG	40-100	Type II kink	101 (14)
	84/85	TAG	5-100	Type II kink	101 (8)
SKC9				N/A	
SK9				N/A	
TK9	72/73	TAG	15-100	Type II kink	73 (11)
SKC8	14	CA	65-100	Unwound step	45 (12)
TK8	30	AA	5-100	Unwound step	54 (12)
	32	AA	10-100	Unwound step	47 (14)

[a] The name convention refers to minicircles described in the text.
[b] The average bend angle and its standard deviation (in parentheses) were calculated between the adjacent 10 bp segments following and preceding the kink and over the time window indicated in column 4.

2. *Torsionally relaxed DNA minicircles*

Three trajectories for Lk = 9 corresponding to the absence of torsional stress were produced for the 94 bp minicircle. The simulate referred to as TK9 (TIP3P, minimal salt) evolves toward a teardrop shape with a single type II kink early in the simulation. In contrast, both simulates with SPC/E, which are SKC9 (150mM KCl) and SK9 (minimal salt), remain unkinked (i.e., the curvature of the DNA molecule is parsimonioulsy distributed along its sequence) over the entire course of the simulations (Fig. 2). The results for Lk = 9 are thus in line with what was simulated in[5] and later in[19], and also with cyclization experiments[2]: kinks are not needed to deal with the bending load typically observed in nucleosomal DNA if it is torsionally relaxed.

We also carried out simulations with the same solvent conditions as in SKC9 but with a sequence truncated at 89 and 99 bp, and with Lk = 9. The goal was to impose a torsional stress intermediary between Lk = 9 and Lk = 10, and between Lk = 8 and Lk = 9, respectively. In these simulates we did not observe any kink formation either, not even temporarily, which supports the assertion made above.

3. *Underwound DNA minicircles*

We carried out MD simulations of underwound minicircles, which were not inquired in[5]. No kink was observed but the negative torsion stress in TK8 and SKC8 was locally absorbed by one bp step (SKC8, Fig. 3) or two bp steps (TK8), respectively CA and twice AA steps (table I), in complete agreement with[4]. As can be seen in Fig. 3, local hotspots of unwound bp step first emerge transiently at diverse positions along the sequence, and in a second phase of the simulation the CA step at position 14 completely unwinds (from 70 ns up to the end of the simulation). These local unwindings are coupled to a significant change in propeller in case of TK8 (Fig. 2) but no other significant change in helical parameter is observed

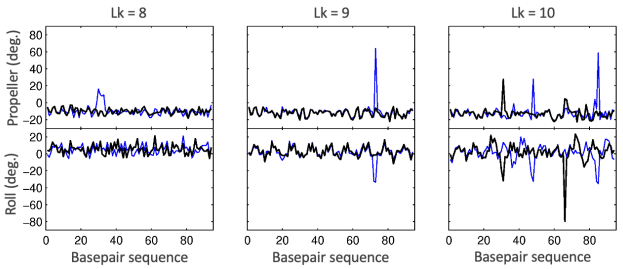

FIG. 2. Average bp propeller (up) and roll (down) in the underwound (left), relaxed (middle) and overwound (right) minicircles. Black: simulation with the SPC/E water model and 150 mM KCl. Blue: simulation with the TIP3P water model and minimal salt. As noted in the text, the increased propeller observed in the underwound minicircle (blue curve) is not due to kinking but to local unwinding.

(e.g. bending or opening). Hence these hotspots help in relieving the global torsional stress[4] but neither kink nor base pair opening appears needed to deal with this bending and torsional load.

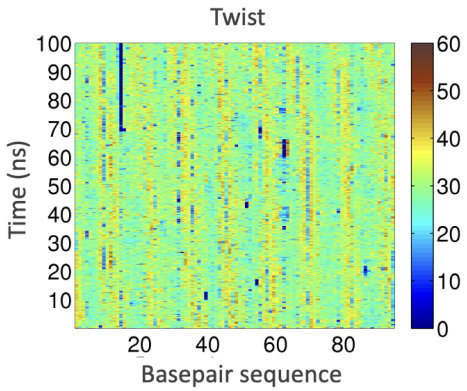

FIG. 3. Time evolution of bp twist in the underwound minicircle (Lk = 8) simulated with the SPC/E water model and 150 mM KCl. Same legends as in Fig. 1. Note one vertical stripe corresponding to complete unwinding of one bp step is observed, while in the simulation with TIP3P and minimal salt (not shown) two vertical stripes were observed.

The lifetime of individual hydrogen bonds in each bp is correlated with the unwinding events described above. For example, in the TK8 simulation the average lifetime of broken hydrogen bonds is 3.3 fs, with two peaks in the distribution of average lifetime along the sequence corresponding to 27.3 ps and 26.0 ps, respectively located where two bp steps are unwound. In the SKC8 simulation, where only one bp step is unwound, the maximum lifetime of broken hydrogen bonds, 12.5 ps, also happens where unwinding happened. And with the combined effect of the transient unwinding events that occur during the first 70 ns the maximum lifetime averaged over the sequence in SKC8 is 0.15 ps, then drops down to only 0.02 ps in the last 30 ns of the trajectory when the CA step at position 14 steadily unwinds and transcient unwinding stops. Thus, the transient unwinding events correlate with an ∼10-fold increase in the maximum lifetime of broken hydrogen bonds.

4. *Conformational substates of DNA backbone*

Non canonical DNA backbone substates were more frequent in the unwound and kinked bp steps than in standard B-form DNA. In the unwound bp steps several backbone dihedrals $(\alpha, \gamma, \varepsilon, \zeta, \xi)$ can be found in some non canonical conformations, but with no clearly preferred substate.

In the kinked bp steps a preference toward the non canonical substate of ε/ζ called BII is observed on at least one of the strands at the position of the kink and also in its neighborhood. The population of BII substates over all ε/ζ instances is less than 15% of the total trajectories on average, see table II. But it is increased to 79% on strand 1 and 25% on strand 2 where the type I kink occurs (step 66) in the SKC10 simulation, and respectively 47% and 70% at the neighboring step 67 (then it drops back to <15%). This is even clearer considering all non canonical substates i.e., not only BII: respectively 90% / 66% at step 66 and 93% / 88% at step 67. For the type II kinks the population of BII conformations is systematically above 50% on both strands, and respectively above 85% when considering all non canonical ε/ζ substates.

Transitions in α/γ DNA backbone dihedrals are less pronounced. In the neighborhood of kinks, the average population of g+/t substates is between 5-10% while it is 1-3% when averaged over all α/γ instances (table II).

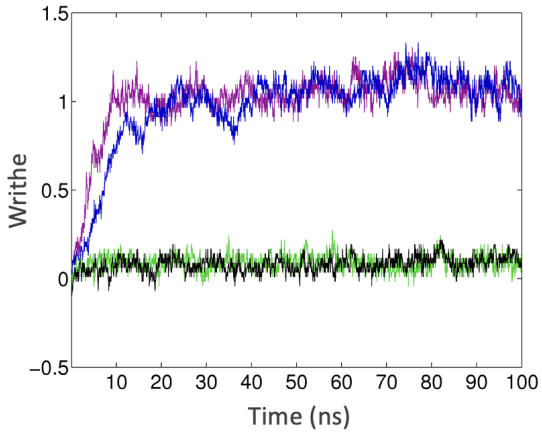

FIG. 4. Time evolution of writhe Wr in the overwound and underwound minicircle simulations. Black: SKC8, Green: TK8, Blue: SKC10, Magenta: TK10.

Apart from where kinks and unwound steps occur (as discussed above), the distribution of backbone dihedral substates is very similar between all current simulations (Table II).

5. *DNA superhelical dynamics*

In this section, the DNA superhelical dynamics is interpreted in term of writhe, rotational register derived from

a Fourier analysis, and molecular projections on dominant eigenvectors derived from a principal component analysis.

The dynamics of the DNA minicircles can be interpreted in term of their global shapes by measuring the time evolution of the writhe number defined by the White formula in the Methods section. A key takeaway from this paper is that all overwound minicircles (Lk = 10) transform the totality of excess twist into an equal amount of writhe. In contrast, underwound minicircles stay planar (Fig. 4). A relationship between DNA writhing and the occurrence of kink was apparent: the first kink event emerges at 10 ns for SKC10 (Fig. 1) and 5 ns for TK10, and in each case this point in time coincides with when the progressive build-up of writhe up to 360° i.e., Wr = 1, is complete. In other words, DNA kinks when Wr = 1. This was observed in all simulations carried out here.

The superhelical dynamics of DNA minicircles can be further interpreted by measuring the time evolution of rotational register obtained from a Fourier analysis in polar coordinates of the roll fluctuation along the minicircle, as described in the Methods section. The occurrence of bp kink has been proposed to lock the rotational register into a small range of values[5], which could be beneficial *in vivo* by preventing arbitrary rotations of DNA molecules during protein-DNA recognition. This was also observed in the current simulations (Fig. 5c). For SKC10 the register stabilizes around a mean value of 118.1° (standard deviation = 8.9°) after the first kink occurs at 10 ns (Fig. 1) and even more clearly after 60 ns when the second kink occurs (mean = 127.5°, standard deviation = 5.8°). This superhelical configuration corresponds to the minor groove of the kinked step facing inward toward the center of the minicircle. Interestingly, the register value at the start of the simulation was 180.8° which placed the minor groove of the step that kinks (step 66, Fig. 1) exactly inward toward the center of the minicircle (Fig. 5b).

When the kinks occur the frequency domain of the Fourier analysis is doubly peaked, meaning two cosine functions are most prevalent when reconstituting the original roll distribution. Fig. 5b shows that both kinks are located at positions of maximum bending toward the center of the minicircle before writhe builds-up (during the first 10 ns, Fig. 4). In these first few ns when kinks have not happen yet, the un-kinked minicircle has a mostly planar superhelix and the frequency domain remains single-peaked (Fig. 5a).

In the relaxed (SKC8) or underwound (SKC9) minicircle simulations, which do not induce any kink, the rotational register drifts more loosely over time with a difference of ∼180° between the beginning and the end of the simulation in SKC8 (mean value = 304.1°, standard deviation = 48.6°). The "flickering" movement of the unwound steps described earlier could explain why the register changes rapidly in the underwound minicircles. Fig. 5c shows that the transient unwinding of bp steps is correlated with some sudden changes in the rotational register. For example, some sudden increases in the register are observed at 20 ns, 25 ns, 45 ns and 65 ns on Fig. 5c, and these correspond to the exact time-lines of spots observed in Fig. 3 respectively at positions 54, 86, 31 and 31. When a CA step at position 14 unwinds and remains unwound in the final 30 ns of the simulation, the register continuously rotates by ∼120° in total across these final 30 ns.

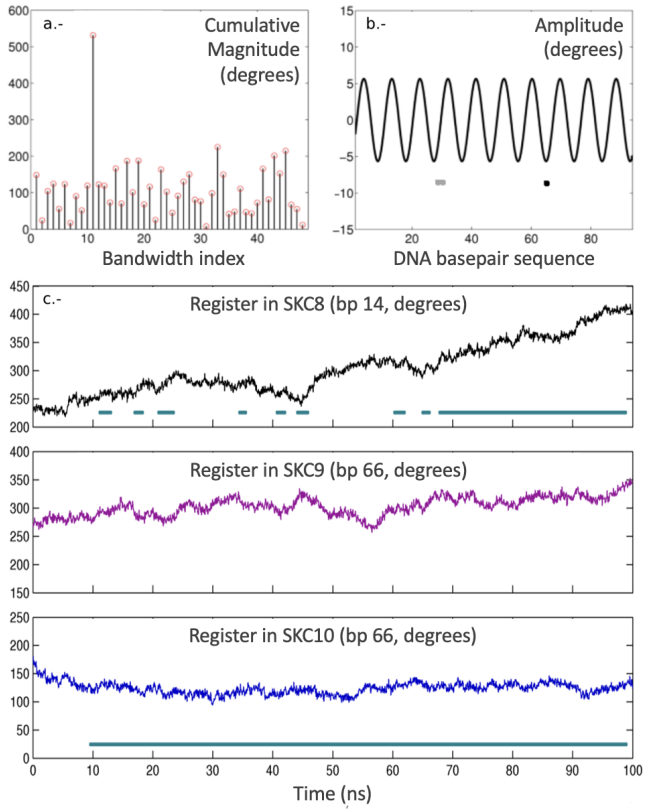

FIG. 5. Fourier series analysis. a.- Frequency domain obtained via discrete Fourier transform in polar coordinates of the bp roll distribution in SKC10 at time t = 5 ns. Note the cosine function corresponding to the first bandwidth index is a constant equal to the average value of roll along the DNA sequence, which shifts all bandwidth indexes by +1. b.- Scaled cosine function corresponding to the 11th bandwidth index in the frequency domain of SKC10 at time t = 5 ns. Positions of kink type II (grey dots) and type I (black dot) are indicated. c.- Phase of the 9th (black), 10th (red), and 11th (blue) scaled cosine function against time for SKC8, SKC9, and SKC10 respectively, which is an approximation to the relative change in rotational register. The phase (in absolute value) was measured at the bp step position indicated on the y-axis. The lines in cyan indicate the time-lines of transient unwinding in SKC8 and of kinking in SKC10.

Finally, a principal component analysis of the kinked minicircles was used to characterize their superhelical dynamics in term of average conformation and maximum displacements away from this average conformation (Fig. 6). When projecting the DNA molecule from its original cartesian coordinates onto its first five eigenvectors in the SKC10 trajectory (after kinks occur i.e., final 90 ns, Fig. 6), the swiss-roll shape described above corresponds to the average conformation (middle frame in Fig. 6). That is, a close-to-straight segment of approximately 36 bp joined to a highly writhed S-shaped segment. At the maximum displacement in either direction onto the first five eigenvectors, the observed shapes resemble what one would obtained respectively from pulling (left hand side in Fig. 6) and pushing (right hand side in Fig. 6) the two ends of an *arrow-bow*.

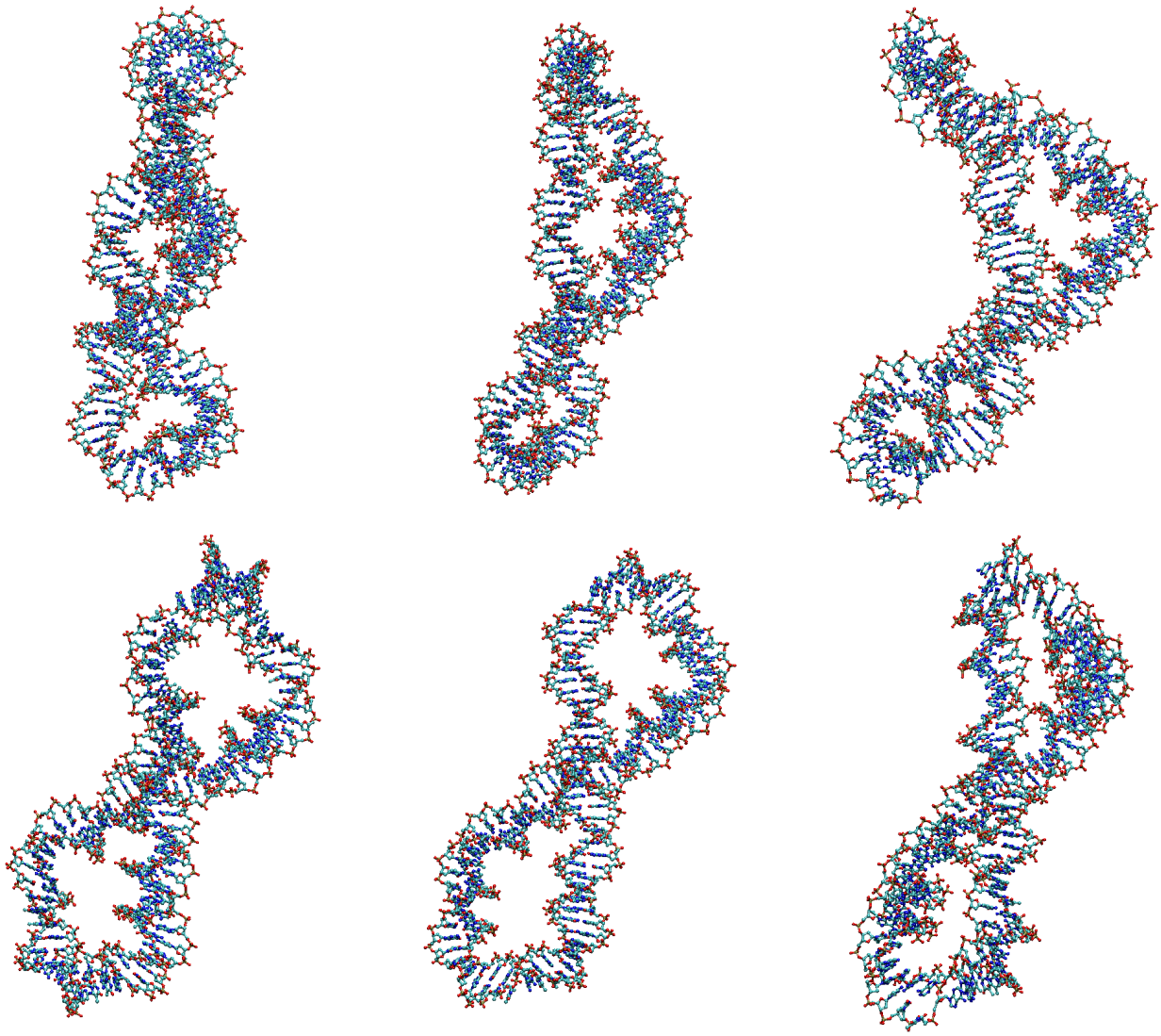

FIG. 6. PCA of the section of the trajectory where kinking occurs in the SKC10 simulation (from 10 to 100 ns). The conformational frames are projections along the first five eigenvectors. The first and second rows are alternative views of an identical structure after rotation by 90° about the vertical. The middle frame corresponds to the average coordinates. Left/right frames correspond to maximum displacement respectively below and above the average coordinates on the first five eigenvectors.

In the characteristic shape obtained by maximum displacement below the average conformation, the overall writhe increases: the long and small segments both wrap around each other (Fig. 6, left), while in the average shape the small segment is straight (Fig. 6, middle). In the analogy of the arrow-bow, this corresponds to the string wrapping around the limb when pulling, because the string *cannot stretch* further, which is also expected in DNA because it is energetically easier to rotate an originally straight DNA superhelix than to stretch it.

In the characteristic shape obtained by maximum displacement above the average conformation, a significant bending is observed for both the long and the small segments, with the latter swept along on the concave side of the long segment (Fig. 6, right). In the analogy of the arrow-bow this corresponds to the string curving parallel to the limb when compressing it. As the two ends are pushed inward, the net distance between the two ends decreases.

The average curvature of the writhed segment is 211.2° when excluding a segment of 10 bp surrounding each kink, and the curvature of the straight segment is 39.3° (Fig. 7). Their standard deviation is similar, 15.4° and 17.0° respectively. The bp twist value in the two segments varies between 20° and 40° on different bp steps (not shown) without clear bp specificity from one time frame to the next. But on average, the bp steps in the writhed segment have a lower twist of 33.9° compared to 34.8° in the straight segment (Fig. 7). The average-twist fluctuation is similar in the short and in the long segments, with a standard deviation of 0.6° and 0.5°, respectively. These results confirm that the short segment of 36 bp preserves a conformational flexibility typical of canonical

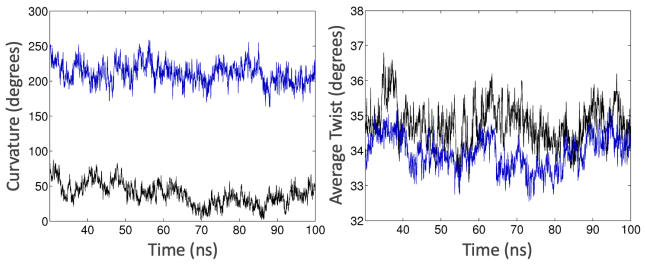

FIG. 7. Curvature and sequence-averaged bp twist in the short segment (black) and long segment (blue) of the swiss-roll shape, i.e. for the section of the trajectory where two kinks are present (from 30 to 100 ns) in the SKC10 simulation. The DNA segment going from bp 35 to 61 (short segment) and the segment composed of bp 1 to 25 + bp 71 to 94 (long segment) were analyzed independently. These were selected to exclude 5 bp on both sides of each kink.

TABLE II. Average proportions of DNA backbone substates.

Simulate[a]	α/γ g−/g+	α/γ others	ε/ζ BI	ε/ζ BII	ε/ζ others
SKC10	0.98	0.02	0.79	0.14	0.07
TK10	0.98	0.02	0.80	0.14	0.06
SKC9	0.99	0.01	0.76	0.17	0.07
SK9	0.99	0.01	0.83	0.12	0.05
TK9	0.99	0.01	0.80	0.13	0.07
SKC8	0.98	0.02	0.88	0.09	0.03
TK8	0.97	0.03	0.87	0.08	0.05

[a] The name convention refers to minicircles described in the text.

B-DNA. Thus, the sharp localized bends flanking this small segment can be interpreted as a mechanism to locally store and release stress so that the 36 bp segment can stay relaxed. The slight writhing and bending of this segment observed in the most extreme deviations during the PCA is typical of B-DNA, and thus support the hypothesis that the superhelical dynamics of nucleosomal DNA can be tighlty controlled and thus can play a key role in gene regulation[1,4].

II. CONCLUSION

All-atom simulations of 94 bp DNA circularized molecules under the influence of torsional stress were analyzed, and the superhelical dynamics was interpreted using Fourier analyses and principal component analyses. Simulations were repeated with different water models and salt concentrations. Every simulation of the overwound minicircles lead to sharp localized bends in the helical axis (kinks). Simulations of the relaxed and underwound minicircles did not generally lead to kinks in the helical structure, but led to some localized unwinding of base pair steps, steadily or transiently. The "flickering" movement of the unwound steps can explain why the rotational register changes more rapidly in underwound DNA. This could be biologically important in making it easier for DNA loops to rotate to bring specific interaction sites into contact.

In the overwound minicircles, kinks are localized at positions of high curvature in the overall superhelical shape of the minicircle and suppress fluctuations in the rotational register. They do not seem associated with unusual transition in the DNA backbone dihedral angles, except for a larger proportion of the so-called BII ε/ζ state. Because the excess twist is almost entirely transformed into writhe by the time the first kinks occur, it is tempting to propose that the build-up of writhe causes the formation of kinks in DNA.

While the underwound minicircles transform the global deficit in twist into local hotspots of fully unwound base pair steps, the overwound minicircles transform the excess twist (all of it) into writhing and give rise to a characteristic shape called swiss-roll, similar to an arrow-bow: a relatively straight segment of 36 bp at each end of which a kink occurs and joined by a highly writhed longer segment. The superhelical dynamics of the kinked, overwound DNA can be summarized as going from superhelical wrapping to superhelical bending i.e., a concerted hinge motion that involves bending the small segment instead of twisting it. In both cases, the range of bending (39° $+/-17^\circ$ for 36 base pair steps) and twisting (34.8° $+/-0.6^\circ$ per base pair step) in the small segment remains within the canonical B-DNA range, even during the maximum displacements observed along the principal components of the conformational eigenspectrum.

These results confirm that stressed DNA molecules are highly heterogeneous along their sequence, with segments designed to locally store and release stress so that nearby segments can stay relaxed. This supports the hypothesis that the superhelical dynamics of nucleosomal DNA can be tightly controlled and thus can play a key role in gene regulation.

ACKNOWLEDGMENTS

The author thanks Richard Lavery, Krystyna Zakrzewska, and John Maddocks, for their suggestions, advices and encouragements during this research.

CONFLICT OF INTEREST

The author (J. D. Curuksu) has no conflicts to disclose.

DATA AVAILABILITY

The data that support the findings of this study, including demos of the PCA superhelical dynamics, are available from the corresponding author upon reasonable request.

REFERENCES

[1] A. L. Pyne, A. Noy, K. H. Main, V. Velasco-Berrelleza, M. M. Piperakis, L. A. Mitchenall, F. M. Cugliandolo, J. G. Beton, C. E. Stevenson, B. W. Hoogenboom, *et al.*, "Base-pair resolution analysis of the effect of supercoiling on DNA flexibility and major groove recognition by triplex-forming oligonucleotides," Nature Communications **12**, 1053 (2021).

[2]Q. Du, A. Kotlyar, and A. Vologodskii, "Kinking the double helix by bending deformation," Nucleic Acids Research **36**, 1120–1128 (2007).
[3]Q. Wang, R. N. Irobalieva, W. Chiu, M. F. Schmid, J. M. Fogg, L. Zechiedrich, and B. M. Pettitt, "Influence of DNA sequence on the structure of minicircles under torsional stress," Nucleic acids research **45**, 7633–7642 (2017).
[4]A. Reymer, K. Zakrzewska, and R. Lavery, "Sequence-dependent response of DNA to torsional stress: a potential biological regulation mechanism," Nucleic acids research **46**, 1684–1694 (2018).
[5]F. Lankaš, R. Lavery, and J. H. Maddocks, "Kinking occurs during molecular dynamics simulations of small DNA minicircles," Structure **14**, 1527–1534 (2006).
[6]L. J. Maher, "DNA kinks available…if needed," Structure **14**, 1479–1480 (2006).
[7]T. E. Cloutier and J. Widom, "Spontaneous sharp bending of double-stranded DNA," Molecular cell **14**, 355–362 (2004).
[8]P. A. Wiggins, T. van der Heijden, F. Moreno-Herrero, A. Spakowitz, R. Phillips, J. Widom, C. Dekker, and P. C. Nelson, "High flexibility of DNA on short length scales probed by atomic force microscopy," Nature Nanotechnology **1**, 137–141 (2006).
[9]S. A. Harris, C. A. Laughton, and T. B. Liverpool, "Mapping the phase diagram of the writhe of DNA nanocircles using atomistic molecular dynamics simulations," Nucleic Acids Research **36**, 21–29 (2007).
[10]J. Curuksu, M. Zacharias, R. Lavery, and K. Zakrzewska, "Local and global effects of strong DNA bending induced during molecular dynamics simulations," Nucleic Acids Research **37**, 3766–3773 (2009).
[11]J. S. Mitchell, C. A. Laughton, and S. A. Harris, "Atomistic simulations reveal bubbles, kinks and wrinkles in supercoiled DNA," Nucleic Acids Research **39**, 3928–3938 (2011).
[12]W. L. Jorgensen, J. Chandrasekhar, J. D. Madura, R. W. Impey, and M. L. Klein, "Comparison of simple potential functions for simulating liquid water," The Journal of Chemical Physics **79**, 926–935 (1983).
[13]H. J. C. Berendsen, J. R. Grigera, and T. P. Straatsma, "The missing term in effective pair potentials," The Journal of Physical Chemistry **91**, 6269–6271 (1987).
[14]R. Lavery, K. Zakrzewska, and H. Sklenar, "Jumna (junction minimisation of nucleic acids)," Computer Physics Communications **91**, 135–158 (1995).
[15]J. H. White, "Self-linking and the Gauss integral in higher dimensions," American Journal of Mathematics **91**, 693 (1969).
[16]D. A. Case, T. A. Darden, T. E. Cheatham, C. L. Simmerling, J. Wang, R. E. Duke, R. Luo, M. Crowley, R. C. Walker, W. Zhang, *et al.*, "Amber 10," Tech. Rep. (University of California, 2008).
[17]R. Lavery, M. Moakher, J. H. Maddocks, D. Petkeviciute, and K. Zakrzewska, "Conformational analysis of nucleic acids revisited: Curves+," Nucleic Acids Research **37**, 5917–5929 (2009).
[18]T. C. Bishop, "Molecular dynamics simulations of a nucleosome and free DNA," Journal of Biomolecular Structure and Dynamics **22**, 673–685 (2005).
[19]M. Pasi, K. Zakrzewska, J. H. Maddocks, and R. Lavery, "Analyzing DNA curvature and its impact on the ionic environment: application to molecular dynamics simulations of minicircles," Nucleic Acids Research **45**, 4269–4277 (2017).
[20]J. Mongan, "Interactive essential dynamics," Journal of Computer-Aided Molecular Design **18**, 433–436 (2004).
[21]F. H. C. Crick and A. Klug, "Kinky helix," Nature **255**, 530–533 (1975).